

High resolution low cost imaging system for particle projection analysis: application to fertilizer centrifugal spreading

This article has been downloaded from IOPscience. Please scroll down to see the full text article.

2002 Meas. Sci. Technol. 13 1087

(<http://iopscience.iop.org/0957-0233/13/7/316>)

View [the table of contents for this issue](#), or go to the [journal homepage](#) for more

Download details:

IP Address: 193.50.47.123

The article was downloaded on 28/07/2010 at 07:43

Please note that [terms and conditions apply](#).

High resolution low cost imaging system for particle projection analysis: application to fertilizer centrifugal spreading

F Cointault¹, P Sarrazin¹ and M Paindavoine²

¹ UMR Cemagref/ENESAD CPAP, 26, Boulevard du Dr Petitjean, BP 87999, F-21079 Dijon Cedex, France

² LE2I, FRE CNRS 2309, Université de Bourgogne, Aile Sciences de l'Ingénieur, BP 47870, 21078 Dijon Cedex, France

E-mail: f.cointault@enesad.fr and paindav@u-bourgogne.fr

Received 11 December 2001, in final form and accepted for publication
9 May 2002

Published 20 June 2002

Online at stacks.iop.org/MST/13/1087

Abstract

This paper describes the design of a high resolution low cost imaging system for the analysis of high speed particle projection. This system, based on a camera and a set of flashes, is used to characterize the centrifugal spreading of fertilizer particles ejected at speeds of $\approx 30 \text{ m s}^{-1}$. Multiexposure images collected with the camera installed perpendicular to the output flow of granules are analysed to estimate the trajectories of the fertilizer granules. Very good results are obtained with the Markov random fields method, in comparison with others.

Keywords: high resolution imaging, high speed motion, trajectories estimation, multiexposure images, centrifugal spreading

(Some figures in this article are in colour only in the electronic version)

1. Introduction

Communication and information technologies have found a wide range of applications in agriculture. This is particularly true with the emergence of the recent concept of 'precision agriculture' (PA)—or site-specific farming—which is based on precise control of all operations (fertilization, pesticide application, seeding, etc) to manage the spatial variability of agricultural fields. These new methodologies allow us to reduce the impact of agriculture on the environment and optimize the crop production yield.

While a lot of research and development work has been focused on localization techniques (such as GPS) and remote sensing for soil and crop characterization, little has been done to adapt agricultural equipment to the accurate control of their operation. In fact, only a few precision fertilization machines are available on the market today. Spreaders based on centrifugal techniques represent 90% of the market for

mineral fertilizer spreaders in Europe. The basic elements of centrifugal spreaders are a hopper for the fertilizer storage and two spreading disks with blades (two or more) spinning at speeds between 700 and 1200 rpm, depending on the manufacturer. The hoppers have a capacity between 300 and 3000 l. The disks are fed with fertilizer near their centre, the granules are accelerated along the blades and ejected with an angular distribution and a velocity distribution. The quality of distribution of the granules on the ground is directly dependent upon these ejection distributions, which vary depending upon numerous parameters such as the nature of the fertilizer, the blade and feeding system geometries, the rotation speed, the mass flow, etc. With conventional agriculture, misadjustment of spreaders based on this technique is often responsible for uneven fertilization, which is harmful to the environment and the yield. In the context of PA, only closed loop regulation systems with appropriate sensors to control the fertilizer distribution would allow an accurate management of the local

fertilization rate. Previous works (Colin 1997, Olieslagers 1997) have shown that the spatial distribution of fertilizer on the ground can be evaluated using the initial conditions of the flight of the granules. Accordingly, a system capable of real-time characterization of the flight of the granules ejected by a spreader would allow a real-time evaluation of the spatial distribution of fertilizer.

This paper presents the design of imaging techniques intended to precisely characterize the spatial distribution of centrifugal spreaders during their operation. The experimental prototype designed to test the techniques and the fast imaging acquisition system for characterizing granule ejection are presented in section 2. Section 3 concerns the image acquisition set-up. Images collected with this system are presented and analysed in section 4. Finally, the evolution of our system and new application domains are discussed.

2. Experimental prototype

2.1. Characteristics of fertilizer output flow and first tests

High speed imaging techniques (Reinke and Tomasini 2000) have been chosen for characterizing this ejection. Prior tests were performed using a high speed camera, HSV 500 NAC, providing a frame rate of 500 fps (frames per second). At this rate, eight images of the same granule throw are collected with, however, a 350×262 pixel image format that cannot provide the resolution required to cover the field of view of ≈ 1 m square necessary to image the whole angular range of projection.

Cameras combining high resolution and high frame rate are scarce and very expensive, and consequently unsuitable for this application. An alternative technique has been developed combining a high resolution slow speed camera in conjunction with a strobe system. This system provides images superimposing successive positions of the same particle throw and has been installed on a spreader prototype.

2.2. Multiexposure imaging

Figure 1 summarizes the principle of the multiexposure imaging technique, also called chronophotography (Edgerton 1983, Winters 1990). The technique is based on the recording of an image superimposing several successive positions of the same fertilizer throw. When N flashes are triggered during a single CCD exposure, the resulting image shows N successive positions of the fertilizer throw. When Δt of an image is high enough so that no overlapping of successive positions occurs, the image can be decomposed into a sequence of N images, simulating the output of a conventional high speed camera.

2.3. Sensor characteristics

2.3.1. Camera. The camera is a Kodak MEGAPLUS ES 1.0/MV low frame rate high resolution digital CCD camera. It operates in single channel mode and allows us to capture up to 15 images s^{-1} with a resolution of over one million pixels with an 8-bit dynamic range. The pixel size is $9.0 \mu_M \times 9.0 \mu_M$ and the active area is $9.07 \text{ mm(H)} \times 9.16 \text{ mm(V)}$.

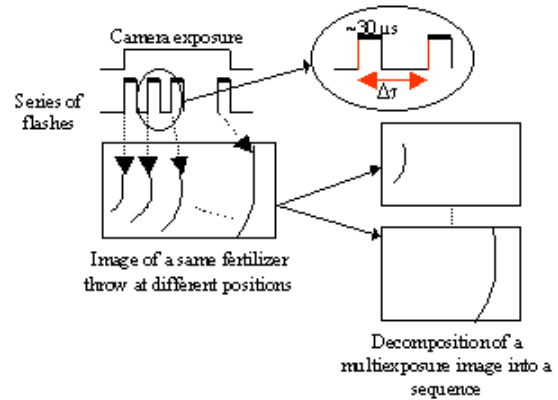


Figure 1. Scheme showing the principle of the multiexposure system.

2.3.2. Lens. The field of view being approximately 1 m square and the height of the camera above the disk being limited to about 1 m, a 8.5 mm focal length Cosmimar C815B lens is fitted on the camera. It gives an angle of view of $40^\circ \times 40^\circ$ with our camera which allows coverage of the desired field of view with a relatively low radial distortion. The maximum aperture is $f = 1.5$.

2.3.3. Strobe unit. No strobe system combining the speed and lighting power required for this application was commercially available, so a special flash unit was built using a series of photographic flashes triggered one after the other over a single camera exposure. The number of flashes determines the maximum number of positions that can be recorded on each image. Eight Vivitar 2800 auto-thyristor flashes (Winters 1990) were modified for very short flash duration in order to prevent blurring from high speed motion of the granules. The flash duration has been reduced to $\approx 30 \mu s$ by exposing the light sensor used in the automatic power adjustment circuit to the direct flash light. The flashes are triggered in a serial mode by a digital controller which also triggers the camera before the first flash is operated. The controller allows the adjustment of the delay between two successive flashes from 128 μs to 8 ms and synchronizes the flash sequence with the disk so that the first flash is always triggered at a given angular position of a blade. The recycling time is programmed into the controller as well and is adjustable from 0.5 to 5 s. A 1 s recycling time has been shown to be the best compromise in order to fully recharge each flash capacitor.

3. Image acquisition set-up

3.1. Background darkening system

The reflection of the light emitted by the flashes on the ground provides an unacceptably bright image background. In order to darken the background, a set of glossy black boards were positioned on the ground at adjustable angles, covering the entire field of view of the camera. The black colour of the boards allows us to reduce the diffuse reflection, while their glossy surface allows us to orient the specular reflection of the light into a direction that does not interfere with the camera, in contrast to matt black surfaces. In addition to controlling the

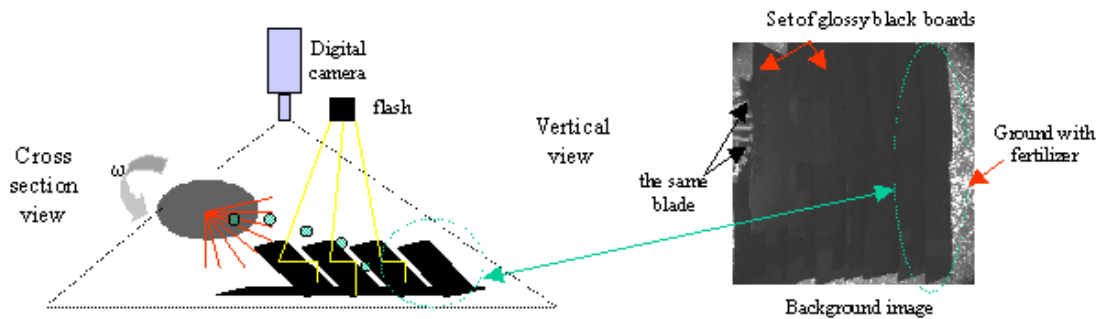


Figure 2. Background control set-up using a set of glossy black boards.

light reflection, this set of boards was useful for evacuating the granules that fall in the vicinity of the spreader as illustrated in figure 2. The first part of this figure shows the background system installed under the spreading disk. The second part presents a background image taken with the camera and the flashes with the black boards partially covering the ground in the field of view. The area covered by the boards is much darker than the ground and all fertilizer granules that fell into this area are hidden.

With further investigation we would have found, perhaps, paints that had suitably diffuse attributes but we did not have the time for that. Moreover, the granule ejection generates some dust that can be easily removed from glossy black boards. Also the background system is just used to increase the contrast in order to cause no mistake between the granules (which are generally clear) and the background.

3.2. Image calibration

Distortions due to the lens have been observed on images collected with the camera. Detailed descriptions of image distortions (especially radial distortion) are given in Beauchemin and Bajcsy (2001). In order to avoid errors in the velocity analyses, a calibration method developed by Heikkilä and Silven (1997) has been used. This method is based on the use of a checkerboard photographed in different positions. An algorithm determines automatically the intersection points of all the black and white squares and then extracts the intrinsic and extrinsic parameters of the camera, used to rectify the images.

The model is based on the 'sténopé' model. If we know the position of a point with 3D 'world' coordinates, the model predicts the position of the image point with 2D 'pixel' coordinates. The 'sténopé' model is based on the colinearity principle, where each point of the object space is projected, by a right line, across the projection centre on the image plane.

In addition to the rectification of the image distortion, the checkerboard is used to spatially calibrate the image acquisition set-up. The checkerboard mounts onto the frame holding the spreading disk in a very precise position. It shows the centre of the disk and provides an x and y scale, each black or white cell measuring exactly $5\text{ cm} \times 5\text{ cm}$. This calibration is an essential step of the image pre-processing because the disk centre coordinates and the blade radius in pixels are required for the trajectory modelling. The rectification shows an error in (X_0, Y_0) coordinates of ≈ 20 pixels on the X axis and 2 pixels

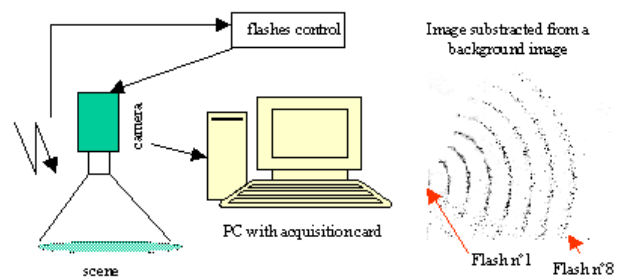


Figure 3. The entire process and a multiexposure image.

on the Y axis. The calibration yields different parameters used in the motion estimation method described in section 4.2.1. These parameters are the centre of the spreading disk and the radius of the blades (in pixels).

4. Image analysis and results

4.1. Multiexposure images

Figure 3 shows an example of a multiexposure image obtained with the NPK 17–17–17 (nitrogen, phosphate, potassium) fertilizer, a flash delay of 4.096 ms , a mass flow of 0.4 kg s^{-1} and a rotation speed of 800 rpm . Figure 3 also shows the entire process too. The camera is positioned vertically at a height of 890 mm above the output flow of granules. The flashes are placed 1500 mm above the plane of the disk and their orientation is optimized to give the best lighting of the granule throws. Two arms allow us to independently adjust the positions of the camera and flash unit.

4.2. Analysis

The sequences of images collected with this system have to be analysed with motion estimation methods in order to determine the motion vectors of the projectiles. We have developed image processing techniques for this purpose. Briefly, the techniques being investigated and characterized upon their capability to determine the velocity field are summarized in the following sections.

4.2.1. *Theoretical modelling of the shape of a throw.* A model of the instantaneous spatial distribution of granules, i.e. a model of the shape of a throw of fertilizer observed at a given time, is adjusted to a single image of a sequence obtained as

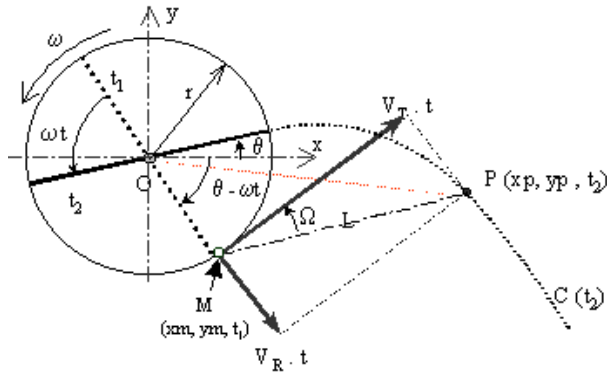


Figure 4. Scheme of a twin-blade disc at two different times t_1 and t_2 .

presented above. This adjustment allows us to determine the average characteristics of the motion of the particles.

Figure 4 presents a scheme of a twin blade spreading disc at two different times: O is the centre of the disc, r is the blade radius, M is the ejection point of a given granule at time t_1 and P is the location of the same particle at time t_2 .

At time t_1 ($t_1 = 0$), a particle is ejected from the blade at the tangential speed $V_t = r\omega$ and radial speed V_r , whereas at time t_2 ($t_2 = t$), the same particle has moved to P and the blade has rotated by an angle ωt . Colin (1997) has shown that, at the ejection and with a flat disk and radial blade configuration, the radial speed is

$$V_r = ar\omega \quad (1)$$

where a is a parameter tied to the dynamic friction coefficient μ of the granule on the blade such that

$$a = \sqrt{(\mu^2 + 1)} - \mu = \tan(\Omega) \quad (2)$$

in its simplified expression, where Ω is the ejection angle. In a simple model that does not take into account the aerodynamic drag of the particle during flight, one can assume that the velocity of the particle remains constant in direction and magnitude in the vicinity of the disk. As such, \vec{MP} carries the direction and magnitude of the granule velocity. The theoretical velocities for each possible position of the granules in the image are given by $((x_p, y_p), (x_M, y_M))$ are respectively the coordinates of points P and M)

$$\begin{aligned} V_x &= ((x_p - x_M)r\omega\sqrt{1 + a^2})/L \\ V_y &= ((y_p - y_M)r\omega\sqrt{1 + a^2})/L \end{aligned} \quad (3)$$

with

$$L = \sqrt{(x_p - x_M)^2 + (y_p - y_M)^2}. \quad (4)$$

The parameter a can be calculated from the multiexposure images which contain sufficient information to infer this parameter, according to different methods. The first method is to determine the ejection angle Ω and then with equation (2) to recover a . This method is not very accurate because of the great uncertainty about the calculation of Ω . The second method consists of using the values of the dynamic friction coefficient given by different authors, like Colin (1997) or Adjroudi (1993), and then to calculate the corresponding a

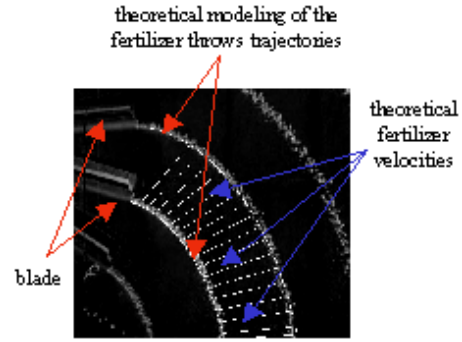


Figure 5. Example of calculation of motion vectors.

parameter. However, in practice as many values of μ exist as there are authors. In accordance with the measurement systems used, the values of this parameter vary in a non-negligible way. This solution has been eliminated.

The third method consists, for each crescent and when varying a for the considered crescent, in finding the value of this parameter giving the intensity maximum. Because we use eight flashes, eight values of a are found and we can then deduce \bar{a} . This technique needs, however, to have constant illumination on the whole crescent, which is not very easy to obtain. A fourth method consists of taking a crescent, varying a and for each value reconstructing the following crescent. Then, we calculate for each reconstructed crescent the gap between the intensities of the real and reconstructed crescents: the lower intensity supposes that the value of a is the best. This last method has been used when comparing the different methods.

After the calculation of a , an approximate motion field is computed using (3). Figure 5 presents a superimposition (rotation speed = 700 rpm) of a real image and a few motion vectors calculated between throws number 4 and 5 with the model.

In the previous case the distance between two successive throws is 125 ± 2 pixels. The difference between observed and calculated motion is about 3–5 pixels, which gives an error between 2.4 and 4%. This error is within the range of the MRF method that can then be used to refine the motion field of each individual granule. This simple technique can approach the actual motion field but does not take into account the variability of ejection velocities. Even if it only provides approximate data, it has been shown to be very useful as a prior motion analysis to initiate more complex refinements.

4.2.2. Refined motion analysis: adaptation of Markov random fields. The MRF technique (Horn and Schunck 1981, Heitz and Bouthemy 1993, Graffigne *et al* 1995, Kardouchi *et al* 1997) on the other hand refines the motion vector locally. The motion vector field calculated as described in the previous section is used as an initialization field for the MRF motion field refinement. The modelling supposes that all the vectors have the same magnitude. This is not true in reality because of the granule's interaction and characteristics. First results have confirmed that the MRF motion analysis leads to a much more accurate motion field as shown in figure 6. Each block of three figures agrees with the same part of the original image.

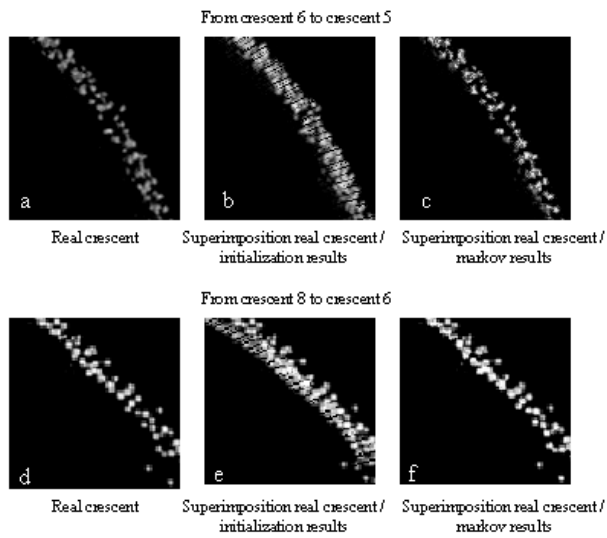


Figure 6. Results for the motion estimation with the MRF method.

Figures 6(b) and (e) represent the superimposition between the original images (6(a) and (d)) and the reconstituted image with initialization vectors. A spreading out of the crescent due to the gap between the original positions and the modelled positions of the pixels does not allow us to recover exactly the real image. Figures 6(c) and (f) represent the superimposition between the original images and the corrected image with ‘Markov’ vectors.

The last superimpositions do not show any notable differences between the original and corrected positions of the pixels, except for the pixel luminance. The real positions of the granules are much more accurately reconstituted with the Markov vectors. This can be seen in figure 6(e) where the initialization vectors do not allow us to obtain the real image. All these results justify the use of the MRF method to correct the direction and the magnitude of the granule velocities. Further improvements of the MRF analysis are being tested at the present time and will allow calculation of the distribution of velocity and direction of ejection.

Table 1 gives instantaneous speeds obtained for the ammonium nitrate fertilizer for three different granules of the same throw. Table 2 gives average speeds (for all the throws) obtained for the NPK 17–17–17 fertilizer. The real speed is calculated manually between two successive images: we first measure the distance, in pixels, between the positions N and $N + 1$ of the same granule. The uncertainty for the distance calculation is 0.20 pixels. Then, knowing the flash delay and the ratio pixels/mm, we deduce the real speed. The ratio depends on the precision of the calibration: it is given with a precision of ± 0.0015 . When taking into account the different uncertainties, the real speed is given at $\pm 0.28 \text{ m s}^{-1}$.

In the two previous cases, the flash delay of 2.048 ms involves a distance between two successive throws of 76 ± 1 pixels. Then the errors detected are of 1–3 pixels, which corresponds to errors between 1.3% and 4% with the modelling method. For the same fertilizer as in figure 7, the errors are a little less, because of the shorter distance.

As shown in the previous tables, the Markov results are better than the results obtained with other methods. The

precision of a centrifugal spreader does not allow us to obtain a very accurate transverse distribution on the ground. In this case, the errors obtained with our modelling technique may be considered as negligible errors in the field. However, since we work in a laboratory we expect to have the most accurate results possible in order to evaluate different motion estimation methods. Even if we cannot evaluate precisely the effects of drag and lift on the fertilizer granules, we can assume that these effects have a very undesirable influence on the projection and then the repartition on the ground. It should be interesting to measure the velocity of the air at ejection in order to take into account this parameter in our model. But in our project we have deliberately limited the study to the determination of the initial conditions of flight of the granules, up to 1.5 m after the ejection. In this case, the effects of drag and lift may be negligible.

The use of the combination of two methods, that is the modelling of the trajectories and the Markov random field (MRF) method, gives very accurate results which can then be used as initial conditions for ballistic models. Table 3 (related to figure 6) gives the ejection angles obtained for three fertilizers (ammonium nitrate (A), KCl (potassium chloride) and NPK 17–17–17).

As we can see in table 3, the parameter a is not a constant during the ejection. Because of this variation, the inferred ejection angle (calculated with equation (2)) varies and decreases when the distance between the granules and the disk increases. This result can be explained by the interactions between the granules, by the lift effect or by the environmental conditions which modify the trajectories of the granules. It appears that, with spherical fertilizers, the ejection angles are nearly similar (around 53°) whereas with an angular fertilizer (i.e. a non-spherical fertilizer) the ejection angle is more important, up to 10° more. With spherical fertilizers, the ejection angle varies 2° between the beginning and the end of the ejection, while with KCl the variation is 5° .

5. Conclusion

The relative high speed movement (near 30 m s^{-1}) of the fertilizer granules needs to use an adapted imaging system in order to recover the granule trajectories. A new technique of image collection has been developed and is based on the use of a high resolution digital camera combined with a set of flashes, which allow us to illuminate the field of view for very short instants and repeat this a few times on the same image. This imaging system allows for the characterization of the initial conditions of flight of the granules in the vicinity of the disk of a centrifugal spreader. The sequence of images obtained with this technique is similar to the output of a high speed camera with, however, the advantage of better spatial resolution and signal to noise ratio, for only a fraction of the cost of a high speed camera.

The decomposed images are then treated with different motion estimation methods, which all need some image corrections and very accurate calibration parameter determination in order to obtain a modelling of the displacement field close to reality.

The first method is simply a modelling of the granule throws needing very accurate determination of the calibration

Table 1. Comparisons between different speeds for the ammonium nitrate fertilizer.

Speeds (m s ⁻¹) C8 and C7 Flash delay = 2.048 ms	$\omega = 800$ rpm Long blades Aperture = 25 mm		
Modelled speed (V_i)	33.54	33.43	33.54
Markov speed (V_m)	34.04	33.92	33.99
Real speed (V_r)	34.02	33.9	33.99
$(V_m - V_r)/V_r$ (in %)	0.06	0.06	0.00
$(V_i - V_r)/V_r$ (in %)	-1.40	-1.39	-1.32

Table 2. Comparisons between different speeds for the NPK 17-17-17 fertilizer.

Average speeds (m s ⁻¹) Flash delay = 4.096 ms	$\omega = 800$ rpm Long blades (325 mm) Aperture = 25 mm	$\omega = 800$ rpm Average blades (275 mm) Aperture = 20 mm
Modelled speed (V_i)	32.61	26.19
Markov speed (V_m)	32.59	26.63
Real speed (V_r)	32.54	26.63
$(V_m - V_r)/V_r$ (in %)	0.15	0.00
$(V_i - V_r)/V_r$ (in %)	0.22	-1.65

Table 3. Ejection angles for the three fertilizers under the same conditions.

	Crescents	a/Ω (deg)		
		KCl	NPK	A
$\omega = 800$ rpm	c8 \rightarrow c7	0.49/ 26.1	0.74/ 36.5	0.71/ 35.37
Short blades (225 mm)	c7 \rightarrow c6	0.52/ 27.47	0.74/ 36.5	0.71/ 35.37
Flash delay = 4.096 ms	c6 \rightarrow c5	0.53/ 27.92	0.74/ 36.5	0.72/ 35.75
Aperture = 20 mm	c5 \rightarrow c4	0.57/ 29.68	0.76/ 37.2	0.72/ 35.75
	c4 \rightarrow c3	0.60/ 30.96	0.76/ 37.2	0.73/ 36.13

parameters. The results were not accurate enough for our application. It appears that the use of theoretical modelling combined with the MRF method, which gives a refinement of the motion estimation, gives very satisfying results. All the results obtained with this image collection system justify widely the use of MRF as a method for the correction of the direction and the speed of the granules. Moreover this technique allows us to treat a large number of granules: the bursting of the particle blocks is then taken into account, so that only the uncontrolled granules give false speeds and directions.

We are now relating the particle trajectory prediction to possible feedback mechanisms to control the parameters of ejection, if possible in real-time.

6. Future works

The present system can be seen as a test system for fertilizer spreading and fertilizer transverse distribution prediction on the ground, in accordance with the adjustments of the spreaders and the physical characteristics of the granules. Moreover it can serve as a reference system for test laboratories, such as the Cemagref of Montoldre, and should then be an additional supply in the real-time determination of the fertilizer transverse repartition. At the present time, such a system cannot be installed on a spreader working in the field. We are working on the design of an image collection system which could be used in the field. This new system is based on single-exposure images which need only an illumination system and a classical camera. The treatment of single-exposure images gives good results for

the determination of the fertilizer angular distribution but does not allow us to recover the trajectories, for the moment.

Then the most important problem concerns the illumination of the scene. In fact, the multiexposure and single-exposure techniques have been tested in a laboratory or in a test centre, with a black uniform background. It is, however, unthinkable to create a black background under the spreading disk in real life, which will not obstruct the granule ejection and will allow us to obtain a uniform background, whatever the soil illumination and nature may be. The problem of sunlight, which can interfere with the image intensity, can be resolved by protecting the camera and the scene in a kind of opaque bubble, but also avoiding disturbing the fertilizer flow.

Another point to study concerns the modifications of two motion estimation methods: the intercorrelation method (Dubois *et al* 2000) and the Gabor filter method (Heeger 1988, Spinei 1998). Since the physical characteristics of the granules are completely random, the blocks used in the intercorrelation method have to be capable of adapting themselves to the sizes of the granules. This does not seem to be possible for the moment, but this is a very interesting point for further research work. Concerning the Gabor filter method, we currently evaluate it with fertilizer images. The advantage of this technique is that it does not need some previous modelling, and it allows us to avoid the errors of the determination of calibration parameters. The improvements, in terms of calculating time, given by Yang and Paindavoine (2000) are not negligible.

References

- Adjroudi R 1993 Comportement d'un flux de particules solides hétérogènes sous l'action d'un lanceur rotatif *Thèse de Doctorat* Institut National Agronomique Paris, Grignon p 170
- Beauchemin S S and Bajcsy R 2001 Calibration of non linear camera lenses *Dagstuhl Castle Seminars (Warden, Germany, March 2000) (Lecture Notes in Computer Science No 2032)* ed R Klette, T Huang and G Gimel (Berlin: Springer) pp 1–22
- Colin A 1997 Etude du procédé d'épandage centrifuge d'engrais minéraux *Thèse de Doctorat de l'UTC de Compiègne* France
- Dubois J, Motyl G J, Fischer V and Fouquet R 2000 System for real time motion measurement *3rd European DSP Education and Research Conf. (Paris)*
- Edgerton H E 1983 *Electronic Flash, Strobe* (Cambridge, MA: MIT Press) pp 24–32
- Graffigne C, Preteux F, Sigelle M, Zerubia J, Perez P and Heitz F 1995 Hierarchical Markov random field models applied to image analysis: a review *Proc. SPIE Conf. on Neural Morphological and Statistic Methods in Image and Signal Processing No 2568 (San Diego, CA, July 1995)* ed E R Dougherty *et al* (Int. Soc. Opt. Eng.) pp 2–18
- Heeger D J 1988 Optical flow using spatio-temporal filters *Int. J. Comput. Vis.* **1** 279–302
- Heikkilä J and Silven O 1997 A four-step camera calibration procedure with implicit image correction *IEEE Computer Society Conf. on Computer Vision and Pattern Recognition (CVPR'97) (San Juan, Puerto Rico)* pp 1106–12
- Heitz F and Bouthemey P 1993 Multimodal estimation of discontinuous optical flow using Markov random fields *IEEE Trans. Pattern Anal. Mach. Intell.* **15** 1217–32
- Horn B K P and Schunck B 1981 Determining optical flow *Artif. Intell.* **17** 185–203
- Kardouchi M, Dipanda A and Legrand L 1997 Motion estimation with Markov random fields using a direct algorithm *SPIE Int. Symp. on Optical Applied Science and Engineering* vol 3101 (Berlin, June 1997) pp 95–103
- Olieslagers R 1997 Fertilizer distribution modelling for centrifugal spreader design *PhD Thesis* University of Louven, Belgium
- Reinke B and Tomasini F 2000 CamRecord, de nouvelles perspectives en vidéo rapide numérique *XVIIIème Colloque National de la Commission d'Imagerie Rapide et Photonique (DGA-Centre technique d'Arcueil)* pp 7–11
- Spinei A 1998 Estimation de mouvement par triades de filtres de Gabor. Application au mouvement d'objets transparents *Thèse de Doctorat* INPG Grenoble, France
- Winters L M 1990 High-Speed Photography with sound triggers *Phys. Teacher* **28** 12
- Yang F and Paindavoine M 2000 Fast motion estimation based on spatio-temporal gabor filters: parallel implementation on multi-DSPs *SPIE 45th Annual Symp. on Optical Science and Technology No 4116 (San Diego, CA, July–Aug. 2000)* ed F T Luk (Int. Soc. Opt. Eng.) pp 454–63